

The random deterioration rate model with measurement error based on the inverse Gaussian distribution

Lia H. M. Morita^a, Vera L. D. Tomazella^b, Pedro L. Ramos^c, Paulo H. Ferreira^c and
Francisco Louzada^c

^aFederal University of Mato Grosso

^bFederal University of São Carlos

^cUniversity of São Paulo

Abstract. In this paper, we introduce the random deterioration rate model with measurement error in order to incorporate the variability among different components. The motivation behind the random variable model is to capture the randomness in the individual differences across the population. This model incorporates only sample uncertainty of the degradation, and no temporal variability is included. The measurement error models appear to overcome this problem. The random rate analysis is based on repeated measurements of failure sizes generated by a degradation process over time in a components population. Some characteristics of the random deterioration rate model based on the inverse Gaussian distribution and subject to measurement error, are examined. We carry out simulation studies to (i) assess the performance of the maximum likelihood estimates obtained through the Gaussian quadrature along with Quasi-Newton optimization method; and (ii) examine the effects of model misspecification on the model selection criteria's performance, as well as on the lifetime prediction's accuracy and precision. The potentiality of the proposed model is illustrated through two real data sets.

1 Introduction

There has been a renewed interest in the development of new lifetime techniques to make reliability assessments. Freitas et al. (2010) pointed out that the reliability assessment of devices is usually based on (accelerated) life tests that register only time-to-failure. Nevertheless, for highly reliable products that exhibit a few or no failures, little information on their reliability is given by such traditional tests. Once most failures occur due to a degradation mechanism at work, for which some features change/degrade over time, one possibility is to monitor the device for some time and estimate its reliability from the changes in performance (degradation) observed during that period.

The random deterioration rate model is a specific stochastic approach commonly applied to corrosion and wear phenomena; see Fenyvesi, Lu and Jack (2004), EPRI (2006) and Huyse and Roodselaar (2010). The motivation behind the random variable model is to capture the randomness in the individual differences across a population. This model incorporates only sample uncertainty of the degradation, and no temporal variability is included. The measurement error models appear to work around this issue. Pandey and Lu (2013) developed a methodology for the estimation of the growth rate parameters in noisy degradation measurement data, whose random sizing error arises due to inspection tools. The authors assigned the exponential and gamma distributions to the deterioration rate, and normal distribution to the measurement errors.

Key words and phrases. Degradation analysis, inverse Gaussian distribution, LASER data, locomotive wheels data, random deterioration rate.

Received March 2019; accepted February 2020.

The primary goal of this paper is to propose a random deterioration rate model based on the inverse Gaussian (IG) distribution and subject to measurement error, in order to account for both sampling and temporal variability associated with a deterioration process. The most commonly used classes of the stochastic process are the gamma and Wiener processes. These two classes have been widely studied and applied in the literature (Peng et al., 2014). Recently, the IG process has been reported as an attractive and flexible stochastic process for degradation modeling by Wang and Xu (2010). Compared with the gamma process, the IG process is more flexible for incorporating random effects and explanatory variables, and is mathematically tractable, especially for certain degradation data (see Wang and Xu, 2010). Alternatively to the above-mentioned stochastic processes, the random deterioration rate model with measurement error based on the IG distribution (instead of the gamma distribution) can be an exciting and useful approach for analyzing real degradation data.

Further, the maximum likelihood estimators are discussed to obtain the estimates for the parameters of the new model. Since the integral involved in the likelihood function does not have a closed-form expression, we considered the Gaussian quadrature method to overcome this problem. Intensive simulation studies are presented under different setups to (i) check the efficiency of our proposed estimators; and (ii) evaluate the effects of model misspecification on the chosen model selection criteria's performance, as well as on the lifetime prediction's accuracy and precision. In the end, we illustrate our proposed methodology to describe the degradation over time of LASER data and locomotive wheels data.

The paper is organized as follows. In Section 2, we review the degradation model. In Section 3, we present the random deterioration rate model. In Section 4, we introduce the random deterioration rate model with measurement error based on the IG distribution and discuss some of its features as well as inference. In Section 5, we show the simulation studies, and in Section 6, we provide the application with two real data sets in the literature. Finally, in Section 7, we give some concluding remarks.

2 The degradation model

In this work, the degradation path of a particular quality characteristic of a product is represented by $D(t)$, and it is a continuous-time stochastic process $\{D(t), t \geq 0\}$, i.e., $D(t)$ is a random quantity $\forall t \geq 0$.

Typically, degradation exhibits an increasing behavior over time, then the product's lifetime T is appropriately defined as the first passage time when $D(t)$ surpasses a threshold ρ , which needs to be fixed in general, that is,

$$T = \inf\{t \geq 0 | D(t) \geq \rho\}. \quad (1)$$

The expression (1) is referred to as the first passage time distribution, which plays a vital role in predicting the remaining useful life as well as in determining optimal maintenance strategies (van Noortwijk, 2009).

The random uncertainties of a degradation process can be featured using different kinds of probabilistic models. In the setting of stochastic processes, we can mention the random deterioration rate model, which is described in the following section.

3 The random deterioration rate model

The simplest stochastic process is defined as a time-dependent function for which the average rate of deterioration per unit time is a random quantity (van Noortwijk, 2009). The random deterioration rate model (or simply, the random rate model) describes the deterioration growth

in a group of components using a linear function and a random parameter. Many other more complicated nonlinear models can be transformed into a linear random deterioration rate model using a time-transformation. In this work, we consider a simple random deterioration rate model as

$$D(t) = Rt \geq 0, \quad \text{with } R > 0, \quad (2)$$

where R is randomly distributed and reflects the uncertain nature of deterioration in a population of identical components.

The random rate model has advantages when the experiment is based on a couple of inspections with no measurement error due to its natural interpretation. Nevertheless, when the number of inspections is large, the individual deterioration rate certainly changes with time, and the inferences for the parameters are inadequate.

4 The random deterioration rate model with measurement error

In engineering problems, generally, data can neither be collected nor registered precisely due to a variety of uncertainties, like human errors, machine errors, or incomplete information (Xiao et al., 2012). Therefore, a source of variability may be added due to measurement errors. The random deterioration rate model is studied following the proposal by Pandey and Lu (2013), in which a measurement error is added to the deterministic model (2) in order to elucidate the source of variability between the measurements from the same individual path. This model is an extension of (2), in which the degradation path of the i th unit at time t is given by

$$D_i(t) = r_i t + \epsilon_i, \quad (3)$$

for $i = 1, 2, \dots, n$, where r_i is the random deterioration rate and ϵ_i is the measurement error.

The model (3) has the same formulation as the general path model (Meeker, Escobar and Lu, 1998), in which the main feature is the randomness between units. Lu and Meeker (1993) presented an approach to analyze noisy degradation data based on the nonlinear mixed-effects regression model assuming a normal distribution with zero mean and positive variance for the measurement error. In this work, ϵ_i belongs to a normal distribution with real mean and positive variance, that is, $\epsilon_i \sim N(\mu_\epsilon, \sigma_\epsilon^2)$, with $-\infty < \mu_\epsilon < \infty$ and $\sigma_\epsilon^2 > 0$.

4.1 Inference for the unknown parameters of the random deterioration rate model

Consider n units being observed at the inspection times $t_{i0} = 0, t_{i1}, \dots, t_{in_i}$, then we have n_i degradation measurements for the i th unit: $D_i(t_{ij}) = d_{ij}$, where $i = 1, 2, \dots, n$ and $j = 0, 1, \dots, n_i$. Then, the model (3) can be rewritten as

$$D_i(t_{ij}) = d_{ij} = r_i t_{ij} + \epsilon_{ij}, \quad (4)$$

where $\epsilon_{ij} \sim N(\mu_\epsilon, \sigma_\epsilon^2)$, with $\mu_\epsilon \in \mathbb{R}$ and $\sigma_\epsilon^2 > 0$.

The analysis is based on a hierarchical modeling used in the Bayesian literature (Kass and Steffey, 1989), which consists of two stages. In the first stage, the deterioration rate r_i is viewed as a latent parameter whose distribution is modeled in the second stage with a hyperparameter vector β . These stages are described below.

- *Stage 1:* The vector $\mathbf{d}_i = (d_{i1}, d_{i2}, \dots, d_{in_i})$ is conditioned on a given r_i , which is regarded as a latent parameter for unit i , with distribution $f(\mathbf{d}_i | r_i)$;
- *Stage 2:* Conditionally on β , the r_i 's constitute an independent and identically distributed (i.i.d.) sample from $f(r_i | \beta)$, and r_i and β are referred to as ‘‘random’’ and ‘‘fixed’’ effects, respectively.

Thus, from conditional independence, the joint density of the data from all units, $\mathbf{d} = (\mathbf{d}_1, \dots, \mathbf{d}_n)$, is a product of specified densities:

$$f(\mathbf{d}|\boldsymbol{\beta}) = \prod_{i=1}^n f(\mathbf{d}_i|\boldsymbol{\beta}),$$

where the unit specific density is a marginal distribution as follows:

$$f(\mathbf{d}_i|\boldsymbol{\beta}) = \int_{R_i} f(\mathbf{d}_i|r_i) f(r_i|\boldsymbol{\beta}) dr_i.$$

The hierarchical procedure is coherent for analyzing noisy data and is not restricted to linear degradation law.

Considering (4) and r_i fixed, the degradation measure $D_{ij} \sim N(\mu_\epsilon + r_i t_{ij}, \sigma_\epsilon^2)$. Hence, the probability density function (p.d.f.) of a measured degradation is given as

$$f(d_{ij}|r_i) = \frac{1}{\sqrt{2\pi}\sigma_\epsilon} \exp\left[-\frac{1}{2\sigma_\epsilon^2}(d_{ij} - \mu_\epsilon - r_i t_{ij})^2\right].$$

From the concept of the hierarchical modeling, the degradation measures \mathbf{d}_i ($i = 1, 2, \dots, n$) are normally distributed with the deterioration rate r_i as a parameter, while r_i itself has the p.d.f. $f(r_i|\boldsymbol{\beta})$.

By using the theorem of total probability, the marginal likelihood function for measurements of an unit i can be written as

$$\begin{aligned} L_i(\mu_\epsilon, \sigma_\epsilon^2, \boldsymbol{\beta}) &= \int_0^\infty \prod_{j=1}^{n_i} \left\{ \frac{1}{\sqrt{2\pi}\sigma_\epsilon} \exp\left[-\frac{1}{2\sigma_\epsilon^2}(d_{ij} - \mu_\epsilon - r_i t_{ij})^2\right] \right\} f(r_i|\boldsymbol{\beta}) dr_i \\ &= L_{1i} \times L_{2i}, \end{aligned} \tag{5}$$

where the first term $L_{1i} = (\frac{1}{\sqrt{2\pi}\sigma_\epsilon})^{n_i}$ does not depend on $\boldsymbol{\beta}$, and the second term $L_{2i} = \int_0^\infty \exp[-\frac{1}{2\sigma_\epsilon^2} \sum_{j=1}^{n_i} (d_{ij} - \mu_\epsilon - r_i t_{ij})^2] f(r_i|\boldsymbol{\beta}) dr_i$ depends on $\boldsymbol{\beta}$ through the integral over r_i .

The likelihood function for a sample of n independent units is the product of the terms $L_1(\mu_\epsilon, \sigma_\epsilon^2, \boldsymbol{\beta}), \dots, L_n(\mu_\epsilon, \sigma_\epsilon^2, \boldsymbol{\beta})$:

$$L(\mu_\epsilon, \sigma_\epsilon^2, \boldsymbol{\beta}) = \prod_{i=1}^n L_i(\mu_\epsilon, \sigma_\epsilon^2, \boldsymbol{\beta}) = \prod_{i=1}^n L_{1i} \times L_{2i}.$$

Hence, the corresponding log-likelihood function is

$$\ell(\mu_\epsilon, \sigma_\epsilon^2, \boldsymbol{\beta}) = \sum_{i=1}^n \log(L_{1i}) + \sum_{i=1}^n \log(L_{2i}). \tag{6}$$

4.2 Lifetime distribution

Considering (1) and (2), the lifetime cumulative distribution function (c.d.f.) is given by

$$F_T(t) = P(D(t) \geq \rho) = P(Rt \geq \rho) = 1 - F_R\left(\frac{\rho}{t}\right), \tag{7}$$

where $F_R(\cdot)$ is the deterioration rate c.d.f.

The corresponding lifetime p.d.f. is obtained by differentiating (7):

$$f_T(t) = \frac{\partial F_T(t)}{\partial t}. \tag{8}$$

The quantiles $t_p, 0 < p < 1$, are obtained from the equation $F_T(t) = p$.

From the nature of degradation data, one may assume a positive-valued distribution for the deterioration rate, r . In this work, we assume an IG distribution for r .

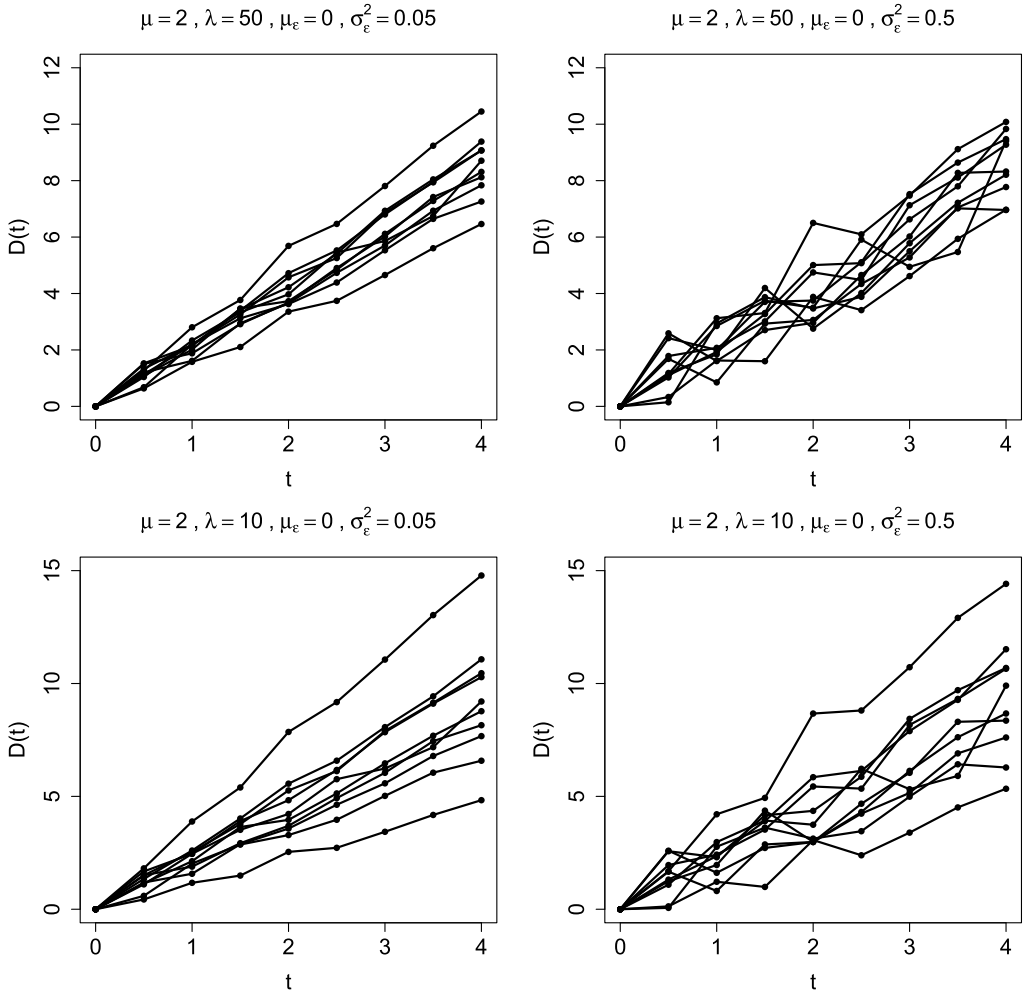


Figure 1 Degradation paths from IG random rate model under different scenarios.

4.3 IG distribution for the random deterioration rate

We shall assume that the r_i 's are an i.i.d. sample from an IG distribution, then we have

$$D_i(t_{ij}) = r_i t_{ij} + \epsilon_{ij}, \quad \text{where } r_i \sim \text{IG}(\mu, \lambda), \tag{9}$$

with $\mu > 0$ being the mean and $\lambda > 0$ is the shape parameter (see Seshadri (2012)). In what follows, we will refer to this model as the IG random deterioration rate model (or simply, the IG random rate model).

Figure 1 shows some degradation paths from the IG random rate model (9). Each plot consists of 10 units being evaluated from 0 up to 4 time units with 8 equidistant intervals. The parameter values are displayed in the graphs. We can see that a decrease in λ leads to an increase in the variability between the paths. While an increase in σ_ϵ^2 leads to an increase in the variability within the paths. Although the paths have increasing behavior, the model formulation allows ups and downs due to measurement error.

4.3.1 Inference. We can rewrite the second term in (5) as

$$L_{2i} = \int_0^\infty \exp \left\{ -\frac{1}{2\sigma_\epsilon^2} \sum_{j=1}^{n_i} (d_{ij} - \mu_\epsilon - r_i t_{ij})^2 \right\} \sqrt{\frac{\lambda}{2\pi r_i^3}} \exp \left\{ -\frac{\lambda(r_i - \mu)^2}{2\mu^2 r_i} \right\} dr_i, \tag{10}$$

which is intractable analytically due to the fact that the integral has no closed-form expression.

The Gaussian quadrature method arises to solve this problem. Such method aims to approximate an integral of a continuous function with respect to a quantity x on X as a weighted sum of this function evaluated at a set of nodes (also called quadrature points):

$$\int_X f(x) dx \approx \sum_{q=1}^Q w_q f(x_q),$$

where the coefficients w_1, \dots, w_Q are the weights and $x_1, \dots, x_Q \in X$ are the nodes.

Some works concerning the use of Gaussian quadrature methods in the regression modeling with random effects include [Pinheiro and Bates \(1995\)](#), [Lesaffre and Spiessens \(2001\)](#), [Carrasco, Ferrari and Arellano-Valle \(2014\)](#), [Crowther et al. \(2016\)](#).

Monte Carlo integration is another alternative method to solve integrals, although one may rewrite (10) so that the integral becomes over another distribution with known parameters. Thus, one can also use the probability integral transform ([Nelson et al., 2006](#)) or the reformulation likelihood method ([Liu and Yu, 2008](#)).

The Gaussian quadrature is faster than the Monte Carlo method in computing numeric integrals. In this work, we obtained the approximation of the integral in (10) by the one-dimensional globally adaptive integrator 15-points Gauss–Kronrod with extrapolation over infinite intervals, which is an extension of the Gaussian quadrature.

Once one has obtained the numerical result for the cited integral, the maximum likelihood estimates (MLEs) can be found by direct maximization of (6) concerning the parameters. Besides, interval estimates and hypothesis tests can be obtained asymptotically.

4.3.2 Lifetime distribution. Considering an IG distribution for the deterioration rate r , the lifetime c.d.f. (7) becomes

$$F_T(t) = \Phi\left(-\sqrt{\frac{\lambda t}{\rho}}\left[\frac{\rho}{t\mu} - 1\right]\right) - \exp\left\{\frac{2\lambda}{\mu}\right\} \Phi\left(-\sqrt{\frac{\lambda t}{\rho}}\left[\frac{\rho}{t\mu} + 1\right]\right), \quad (11)$$

where $\Phi(\cdot)$ is the standard normal c.d.f.

Moreover, the lifetime p.d.f. in (8) becomes

$$f_T(t) = \exp\left\{-\frac{\lambda(-\mu t + \rho)^2}{2\mu^2 t \rho}\right\} \sqrt{\frac{\lambda}{2\pi \rho t}}.$$

Therefore, the meantime to failure (MTTF) is given by

$$\text{MTTF} = \frac{\rho(\mu + \lambda)}{\mu\lambda}.$$

[Peng and Tseng \(2009\)](#) gave special attention to the MTTF estimation, which can be significantly affected by model misspecification in the degradation analysis.

Finally, the quantiles of (11) have no analytical form, so we resort to numerical root-finding methods to find approximate solutions.

5 Simulation studies

In this section, we present the main results obtained from simulation studies aimed at (i) verifying properties of the MLEs of the model parameters (Section 5.1); and (ii) investigating the effects of model misspecification on the appropriateness of the chosen model selection criteria, as well as on the accuracy and precision of the lifetime prediction (Section 5.2).

All the computations and simulations were done using the Ox programming language ([Doornik, 2009](#)).

Table 1 MLEs, 95% CPs and MSEs under different σ_ϵ^2 values

| n | Parameter | $\sigma_\epsilon^2 = 0.05$ | | | $\sigma_\epsilon^2 = 0.5$ | | |
|-----|---------------------|----------------------------|--------|--------------------|---------------------------|--------|-----------|
| | | MLE | 95% CP | MSE | MLE | 95% CP | MSE |
| 10 | $\mu(2)$ | 1.9988 | 0.9130 | 0.0153 | 1.9997 | 0.9230 | 0.0184 |
| | $\lambda(50)$ | 73.8300 | 0.9620 | 2946.0000 | 78.7930 | 0.9550 | 5627.0000 |
| | $\mu_\epsilon(0)$ | 0.0001 | 0.9370 | 0.0024 | 0.0008 | 0.9380 | 0.0234 |
| | σ_ϵ^2 | 0.0495 | 0.9300 | 0.0001 | 0.4951 | 0.9300 | 0.0055 |
| 20 | $\mu(2)$ | 2.0022 | 0.9300 | 0.0080 | 1.9992 | 0.9230 | 0.0101 |
| | $\lambda(50)$ | 59.8800 | 0.9670 | 630.8600 | 61.4230 | 0.9700 | 802.8100 |
| | $\mu_\epsilon(0)$ | 0.0006 | 0.9520 | 0.0012 | 0.0002 | 0.9500 | 0.0113 |
| | σ_ϵ^2 | 0.0499 | 0.9530 | 2×10^{-5} | 0.4981 | 0.9400 | 0.0028 |
| 30 | $\mu(2)$ | 1.9992 | 0.9450 | 0.0052 | 2.0013 | 0.9380 | 0.0067 |
| | $\lambda(50)$ | 56.0010 | 0.9650 | 269.3100 | 55.8910 | 0.9700 | 292.9000 |
| | $\mu_\epsilon(0)$ | 4×10^{-5} | 0.9570 | 0.0007 | -0.0012 | 0.9480 | 0.0078 |
| | σ_ϵ^2 | 0.0500 | 0.9490 | 2×10^{-5} | 0.4995 | 0.9490 | 0.0019 |
| 50 | $\mu(2)$ | 1.9997 | 0.9530 | 0.0030 | 2.0008 | 0.9600 | 0.0036 |
| | $\lambda(50)$ | 53.2550 | 0.9560 | 124.8400 | 53.3090 | 0.9670 | 148.6100 |
| | $\mu_\epsilon(0)$ | -0.0031 | 0.9300 | 0.0007 | -0.0012 | 0.9590 | 0.0046 |
| | σ_ϵ^2 | 0.0506 | 0.9130 | 3×10^{-5} | 0.4993 | 0.9440 | 0.0012 |
| 100 | $\mu(2)$ | 1.9989 | 0.9470 | 0.0016 | 1.9989 | 0.9590 | 0.0019 |
| | $\lambda(50)$ | 52.0270 | 0.9600 | 57.7280 | 51.7530 | 0.9520 | 69.1820 |
| | $\mu_\epsilon(0)$ | -0.0023 | 0.9160 | 0.0003 | 0.0013 | 0.9490 | 0.0023 |
| | σ_ϵ^2 | 0.0509 | 0.8920 | 2×10^{-5} | 0.5008 | 0.9500 | 0.0005 |

5.1 Parameter recovery study

The first simulation study was conducted based on the generation of 1000 artificial data sets from the IG random rate model (9) with five different sample sizes: $n = 10, 20, 30, 50$ and 100. The components were evaluated from 0 up to 4 time units with 10 equidistant intervals. The mean parameters were kept fixed: $\mu = 2$ and $\mu_\epsilon = 0$, while the shape and scale parameters assumed different values: $\lambda = 20$ or 50, and $\sigma_\epsilon^2 = 0.05$ or 0.5. Such parameter values give degradation paths with similar features to the LASER data set (Meeker and Escobar, 1998), in which the variation of λ and σ_ϵ^2 describes a source of variation among and within the paths, respectively.

The MLEs of the model parameters, the coverage probabilities at level 95% (95% CPs), and the mean square errors of the MLEs (MSEs) under different λ and σ_ϵ^2 values are discussed.

Table 1 displays the MLEs, 95% CPs and MSEs under $\sigma_\epsilon^2 = 0.05$ and $\sigma_\epsilon^2 = 0.5$, from which we conclude that, in general, the MLEs are close to the corresponding true values. Regarding the 95% CPs, we notice that, when $\sigma_\epsilon^2 = 0.05$ and n increases, the 95% CPs for μ and λ are closer to 95% and the 95% CPs for μ_ϵ and σ_ϵ^2 are closer to 90%, which is acceptable; and when $\sigma_\epsilon^2 = 0.5$ and n increases, all 95% CPs are closer to the nominal value (95%). Moreover, the MSEs are lower as n increases, for different σ_ϵ^2 values.

Still, regarding the 95% CP values close to 90% for $\sigma_\epsilon^2 = 0.05$, we can see that the lower the σ_ϵ^2 , the smaller the variability within the paths; meanwhile, the larger the sample size, the higher the variability among the paths. Therefore, the MLEs of μ_ϵ and σ_ϵ^2 have a small bias even for large sample sizes.

Table 2 exhibits the MLEs, 95% CPs and MSEs under $\lambda = 20$ and $\lambda = 50$, from which we conclude that the MLEs are close to the corresponding true values for different λ values.

Table 2 MLEs, 95% CPs and MSEs under different λ values

| n | Parameter | $\lambda = 20$ | | | $\lambda = 50$ | | |
|-----|--------------------------|----------------|--------|----------|----------------|--------|-----------|
| | | MLE | 95% CP | MSE | MLE | 95% CP | MSE |
| 10 | $\mu(2)$ | 2.0016 | 0.9240 | 0.0396 | 1.9997 | 0.9230 | 0.0184 |
| | λ | 29.8610 | 0.9610 | 567.2100 | 78.7930 | 0.9550 | 5627.0000 |
| | $\mu_\epsilon(0)$ | 0.0011 | 0.9400 | 0.0236 | 0.0008 | 0.9380 | 0.0234 |
| | $\sigma_\epsilon^2(0.5)$ | 0.4951 | 0.9290 | 0.0055 | 0.4951 | 0.9300 | 0.0055 |
| 20 | $\mu(2)$ | 1.9977 | 0.9160 | 0.0222 | 1.9992 | 0.9230 | 0.0101 |
| | λ | 24.3220 | 0.9690 | 114.4200 | 61.4230 | 0.9700 | 802.8100 |
| | $\mu_\epsilon(0)$ | 0.0003 | 0.9510 | 0.0113 | 0.0002 | 0.9500 | 0.0113 |
| | $\sigma_\epsilon^2(0.5)$ | 0.4981 | 0.9400 | 0.0028 | 0.4981 | 0.9400 | 0.0028 |
| 30 | $\mu(2)$ | 2.0021 | 0.9400 | 0.0145 | 2.0013 | 0.9380 | 0.0067 |
| | λ | 22.2440 | 0.9660 | 44.0760 | 55.8910 | 0.9700 | 292.9000 |
| | $\mu_\epsilon(0)$ | -0.0011 | 0.9480 | 0.0078 | -0.0012 | 0.9480 | 0.0078 |
| | $\sigma_\epsilon^2(0.5)$ | 0.4995 | 0.9510 | 0.0017 | 0.4995 | 0.9490 | 0.0019 |
| 50 | $\mu(2)$ | 2.0008 | 0.9500 | 0.0081 | 2.0008 | 0.9600 | 0.0036 |
| | λ | 21.2260 | 0.9650 | 21.5060 | 53.3090 | 0.9670 | 148.6100 |
| | $\mu_\epsilon(0)$ | -0.0011 | 0.9570 | 0.0046 | -0.0012 | 0.9590 | 0.0046 |
| | $\sigma_\epsilon^2(0.5)$ | 0.4993 | 0.9440 | 0.0012 | 0.4993 | 0.9440 | 0.0012 |
| 100 | $\mu(2)$ | 1.9981 | 0.9640 | 0.0041 | 1.9989 | 0.9590 | 0.0019 |
| | λ | 20.6555 | 0.9530 | 10.4000 | 51.7530 | 0.9520 | 69.1820 |
| | $\mu_\epsilon(0)$ | 0.0013 | 0.9470 | 0.0023 | 0.0013 | 0.9490 | 0.0023 |
| | $\sigma_\epsilon^2(0.5)$ | 0.5008 | 0.9510 | 0.0005 | 0.5008 | 0.9500 | 0.0005 |

Furthermore, as n increases, the 95% CPs are closer to the nominal value and the MSEs are lower.

5.2 Misspecification study

In this subsection, we perform a second simulation study to demonstrate the robustness of the proposed model under model misspecification. Mainly, 1000 simulations were carried out using the QUADPACK routine (Piessens et al., 2012) along with the Quasi-Newton optimization method via BFGS algorithm available in Ox software (Doornik, 2009).

Firstly, we consider a special case of the IG random rate model (9), where samples of size $n = 10, 20, 30, 50$ and 100 , for the deterioration rate r_i ($i = 1, 2, \dots, n$), are simulated from an IG distribution with parameters $\mu = 2$ and $\lambda = 50$, but we will also assume that the data come from a random deterioration rate model based on the gamma distribution (Pandey and Lu, 2013), referred to as the gamma random rate model along the section, which is given by

$$D_i(t_{ij}) = r_i t_{ij} + \epsilon_{ij}, \quad \text{where } r_i \sim \text{Gamma}(\varphi, \nu), \tag{12}$$

with $\varphi > 0$ being the shape parameter, $\nu > 0$ is the scale parameter, and the p.d.f. of r_i is $f(r_i|\varphi, \nu) = \frac{r_i^{\varphi-1}}{\Gamma(\varphi)\nu^\varphi} \exp\{-\frac{r_i}{\nu}\}$.

Secondly, we consider a particular case of the gamma random rate model (12), where samples of size $n = 10, 20, 30, 50$ and 100 , for r_i ($i = 1, 2, \dots, n$), are drawn from a gamma distribution with parameters $\varphi = 26.5760$ and $\nu = 0.0767$, but again, we will also suppose that the data come from an IG random rate model with parameters μ and λ .

It is worth noting that the parameters of both models were set so that their observed mean and variance values are approximately the same (2 and 0.16, respectively).

In both cases, the model chosen as the best fit was the one which provided the lower AIC (Akaike information criterion) (Sakamoto, Ishiguro and Kitagawa, 1986) value. We also

Table 3 The percentage (%) of times each random rate model is selected as the best one according to the AIC statistic, for different σ_ϵ^2 values

| True model | n | $\sigma_\epsilon^2 = 0.05$ | $\sigma_\epsilon^2 = 0.5$ |
|-------------------|-----|----------------------------|---------------------------|
| IG random rate | 10 | 58.50 | 58.10 |
| | 20 | 54.90 | 58.30 |
| | 30 | 57.70 | 55.70 |
| | 50 | 60.40 | 59.10 |
| | 100 | 66.30 | 60.70 |
| Gamma random rate | 10 | 52.50 | 51.70 |
| | 20 | 53.30 | 54.20 |
| | 30 | 58.40 | 58.30 |
| | 50 | 58.90 | 57.80 |
| | 100 | 62.30 | 64.80 |

consider two different scenarios for the data dispersion: $\sigma_\epsilon^2 = 0.05$ and $\sigma_\epsilon^2 = 0.5$, which describe, respectively, low and large sources of variability within the paths.

The obtained results are displayed in Table 3, revealing that model selection/discrimination with AIC showed a high percentage of correctly classified samples (for both models, this percentage is higher than 50%). Observe also that the AIC performance is still better for the IG random rate model in the presence of small samples (i.e., when $n \leq 20$).

We also performed the present simulation study by considering the BIC (Bayesian or Schwarz information criterion) (Schwarz, 1978). Nevertheless, since both models have the same number of parameters, the results led to similar conclusions and were omitted here.

Finally, the estimation results shown in Table 4 indicate that both IG and gamma random rate models are equally robust to model misspecification, with quite similar MLEs, MSEs and 95% CIs of the lifetime 10th, 50th and 80th percentiles and MTTF. Note that in order to save space, we only present the results for $\sigma_\epsilon^2 = 0.05$ (in fact, $\sigma_\epsilon^2 = 0.5$ led to the same findings).

6 Application

For the analysis and comparison purposes, we bring forward the gamma random rate model (12).

In the application with the LASER data (Section 6.1) and locomotive wheels data (Section 6.2), the MLEs were obtained by the Quasi-Newton optimization method via Broyden–Fletcher–Goldfarb–Shanno (BFGS) algorithm (Broyden, 1970). The values used to initialize this algorithm in the IG random rate model were achieved by the following steps:

1. Let $\mu^{(0)}, \lambda^{(0)}, \mu_\epsilon^{(0)}$ and $\sigma_\epsilon^{2(0)}$ be the starting values of $\mu, \lambda, \mu_\epsilon$ and σ_ϵ^2 , respectively;
2. For each degradation path, fit the model (9) using the method of least squares, thus obtaining the observed degradation rates $\hat{r}_1, \hat{r}_2, \dots, \hat{r}_n$ of r_1, r_2, \dots, r_n , respectively;
3. Suppose that $\hat{r}_1, \hat{r}_2, \dots, \hat{r}_n \stackrel{\text{iid}}{\sim} \text{IG}(\mu, \lambda)$, then $\mu^{(0)}$ and $\lambda^{(0)}$ are taken as the MLEs of μ and λ , respectively;
4. Obtain the residuals $e_{ij} = D_i(t_{ij}) - \hat{r}_i t_{ij}$ ($i = 1, 2, \dots, n$ and $j = 1, 2, \dots, n_i$), then $\mu_\epsilon^{(0)}$ and $\sigma_\epsilon^{2(0)}$ are taken, respectively, as the sample mean and sample variance of the residuals.

The starting values for the gamma random rate model can be obtained analogously.

Although the Ox software was used to conduct almost all these real data analyses, and the R software (R Core Team R, 2018) was also considered to perform specific tasks, such as

Table 4 MLEs, 95% CPs and MSEs of the lifetime percentiles and MTTF under model misspecification and considering true parameter values in Gamma random rate model as $t_{0,1} = 3.9091$, $t_{0,5} = 4.9691$, $t_{0,8} = 5.8824$ and $MTTF=5.0988$, and true parameter values in IG random rate model as $t_{0,1} = 3.9536$, $t_{0,5} = 5.0997$, $t_{0,8} = 6.0278$ and $MTTF=5.2$

| Fitted model/True model | n | Quantity | Gamma random rate | | | IG random rate | | | |
|-------------------------|-------------------|-----------|-------------------|---------|--------|----------------|---------|--------|--------|
| | | | MLE | 95% CP | MSE | MLE | 95% CP | MSE | |
| IG random rate | 10 | $t_{0,1}$ | 3.9944 | 0.9120 | 0.1025 | 4.0496 | 0.8950 | 0.1202 | |
| | | $t_{0,5}$ | 5.0348 | 0.9020 | 0.1131 | 5.1114 | 0.9190 | 0.1026 | |
| | | $t_{0,8}$ | 5.8714 | 0.8820 | 0.2294 | 5.9667 | 0.8750 | 0.2045 | |
| | | MTTF | 5.1126 | 0.8970 | 0.1206 | 5.2018 | 0.9120 | 0.1098 | |
| | 20 | $t_{0,1}$ | 3.9390 | 0.9330 | 0.0511 | 4.0015 | 0.9230 | 0.0579 | |
| | | $t_{0,5}$ | 5.0172 | 0.9250 | 0.0540 | 5.1014 | 0.9190 | 0.0550 | |
| | | $t_{0,8}$ | 5.8865 | 0.9190 | 0.1052 | 5.9885 | 0.9020 | 0.1045 | |
| | | MTTF | 5.1094 | 0.9160 | 0.0563 | 5.1956 | 0.91700 | 0.0586 | |
| | 30 | $t_{0,1}$ | 3.9158 | 0.9530 | 0.0295 | 3.9895 | 0.9240 | 0.0377 | |
| | | $t_{0,5}$ | 5.0025 | 0.9360 | 0.0326 | 5.1024 | 0.9310 | 0.0326 | |
| | | $t_{0,8}$ | 5.8791 | 0.9100 | 0.0702 | 6.0008 | 0.9340 | 0.0624 | |
| | | MTTF | 5.0957 | 0.9330 | 0.0350 | 5.1982 | 0.9340 | 0.0345 | |
| | 50 | $t_{0,1}$ | 3.9012 | 0.955 | 0.0191 | 3.9727 | 0.9440 | 0.0223 | |
| | | $t_{0,5}$ | 4.9985 | 0.9350 | 0.0209 | 5.1006 | 0.9570 | 0.0198 | |
| | | $t_{0,8}$ | 5.8844 | 0.9190 | 0.0430 | 6.0123 | 0.9530 | 0.0356 | |
| | | MTTF | 5.0930 | 0.9320 | 0.0221 | 5.1984 | 0.9550 | 0.0207 | |
| | 100 | $t_{0,1}$ | 3.9001 | 0.9490 | 0.0100 | 3.9587 | 0.9220 | 0.0128 | |
| | | $t_{0,5}$ | 5.0013 | 0.9270 | 0.0109 | 5.0981 | 0.9270 | 0.0116 | |
| | | $t_{0,8}$ | 5.8899 | 0.9310 | 0.0199 | 6.0206 | 0.9390 | 0.0202 | |
| | | MTTF | 5.0959 | 0.93700 | 0.0107 | 5.1978 | 0.9350 | 0.0121 | |
| | Gamma random rate | 10 | $t_{0,1}$ | 4.0109 | 0.8900 | 0.1038 | 4.0632 | 0.8680 | 0.1212 |
| | | | $t_{0,5}$ | 5.0045 | 0.8940 | 0.1070 | 5.0807 | 0.9140 | 0.1012 |
| | | | $t_{0,8}$ | 5.8555 | 0.8940 | 0.2228 | 5.9552 | 0.8830 | 0.2026 |
| | | | MTTF | 5.1235 | 0.9020 | 0.1207 | 5.2046 | 0.9200 | 0.1103 |
| 20 | | $t_{0,1}$ | 3.9570 | 0.9080 | 0.0510 | 4.0161 | 0.9060 | 0.0587 | |
| | | $t_{0,5}$ | 4.9853 | 0.9250 | 0.0508 | 5.0694 | 0.9150 | 0.0551 | |
| | | $t_{0,8}$ | 5.8689 | 0.9270 | 0.1020 | 5.9763 | 0.9100 | 0.1038 | |
| | | MTTF | 5.1099 | 0.9240 | 0.0564 | 5.1982 | 0.9250 | 0.0588 | |
| 30 | | $t_{0,1}$ | 3.9350 | 0.9420 | 0.0290 | 4.0047 | 0.9030 | 0.0384 | |
| | | $t_{0,5}$ | 4.9701 | 0.9430 | 0.0306 | 5.0699 | 0.9310 | 0.0332 | |
| | | $t_{0,8}$ | 5.8600 | 0.9140 | 0.0678 | 5.9879 | 0.9420 | 0.0623 | |
| | | MTTF | 5.0957 | 0.9350 | 0.0350 | 5.2006 | 0.9420 | 0.0347 | |
| 50 | | $t_{0,1}$ | 3.9215 | 0.9430 | 0.0183 | 3.9878 | 0.9270 | 0.0229 | |
| | | $t_{0,5}$ | 4.9672 | 0.9380 | 0.0200 | 5.0677 | 0.9440 | 0.0205 | |
| | | $t_{0,8}$ | 5.8672 | 0.9260 | 0.0434 | 6.0004 | 0.9600 | 0.0353 | |
| | | MTTF | 5.0947 | 0.9390 | 0.0228 | 5.2014 | 0.9600 | 0.0205 | |
| 100 | | $t_{0,1}$ | 3.9192 | 0.9380 | 0.0094 | 3.9747 | 0.9030 | 0.0128 | |
| | | $t_{0,5}$ | 4.9698 | 0.9500 | 0.0093 | 5.0657 | 0.9240 | 0.0125 | |
| | | $t_{0,8}$ | 5.8736 | 0.9470 | 0.0187 | 6.0101 | 0.9530 | 0.0201 | |
| | | MTTF | 5.0975 | 0.9490 | 0.0103 | 5.2020 | 0.9490 | 0.0119 | |

the construction of the probability-probability (P-P) plots and the Anderson-Darling (AD) goodness-of-fit (GOF) tests of the observed degradation rates.

The Ox and R codes that we have developed for the complete analysis of the LASER data are available as Supplemental Material ((Morita et al., 2020)).

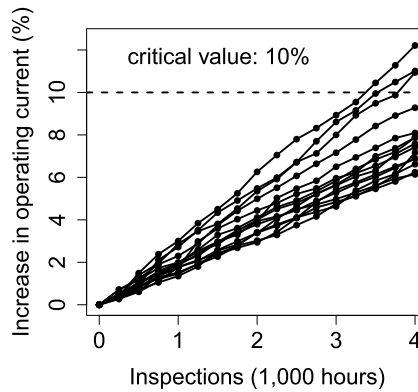


Figure 2 Degradation paths from the LASER data.

6.1 The LASER data

Some gadgets for light amplification by stimulated emission of radiation, named LASER, exhibit degradation over time, which results in a reduction of the emitted light. This lightness can be kept quite constant with an increase in the operating current. When this current achieves a very high value, it is considered that the unit has failed. Meeker and Escobar (1998) showed a study with degradation data of 15 LASER units from Gallium arsenide (GaAs) kind, with observations made at 4000 hours of operation, with 16 equidistant time intervals. The degradation measure for each LASER unit is the percent increase in the current overtime, concerning the nominal current, and a unit is considered to have failed when its degradation measure achieves 10%. Figure 2 displays the degradation paths, indicating the critical value associated with the failure. It is worth pointing out that Meeker and Escobar (1998) first analyzed these LASER data under an approximate degradation analysis. The authors first fitted straight lines through the origin for each degradation path, then obtained the pseudo times to failure. Thereby, they proceeded with a likelihood analysis under a Weibull distribution for the failure times and made inferences on the time-to-failure distribution.

Table 5 displays the MLEs, the standard errors of the MLEs (SEs) and the 95% confidence intervals (95% CIs) of the parameters under the IG random rate model (9) and the gamma random rate model (12), based on the LASER data. From this table, we conclude that the MLEs of μ_ϵ and σ_ϵ^2 are the same in both models, as well as their SEs and 95% CIs. Moreover, the measurement errors are slightly shifted to the right, assuming more positive than negative values. For illustrative purposes, each unit time stands for 1000 hours of operation, so the MLEs of μ and λ in model (9), as well as the MLE of ν in model (12), have to be divided by 1000 for practical interpretation.

Table 6 presents the model selection criteria AIC and BIC, which both indicate the IG random rate model as the best one that fitted the LASER data, as its AIC and BIC values are the lowest. Nevertheless, the difference between the AIC (BIC) value for the IG random rate model and the AIC (BIC) value for the gamma random rate model is $0.825 < 2$, which, according to the rule of thumb suggested by Burnham and Anderson (2002, page 70) (Raftery, 1995, Table 6), shows weak evidence for the superiority of the proposed model over the conventional one. Therefore, both IG and gamma random rate models are plausible for describing this data set.

Additionally, we resort to the P–P plot and the AD test of the observed degradation rates to evaluate the GOF of the IG and gamma random rate models. The observed degradation rates are obtained from a simple linear regression model without intercept fitted to each degradation path. The GOF test is verified according to the proposal of Villaseñor and Gonzalez-Estrada (2015), which consists in transforming the IG variables into gamma variables and

Table 5 MLEs, SEs and 95% CIs of the model parameters based on the LASER data

| Model | Parameter | MLE | SE | 95% CI |
|-------------------|---------------------|---------|---------|--------------------|
| IG random rate | μ | 2.0418 | 0.1094 | [1.8275; 2.2562] |
| | λ | 47.9760 | 17.5780 | [13.5240; 82.4290] |
| | μ_ϵ | 0.0131 | 0.0279 | [-0.0416; 0.0677] |
| | σ_ϵ^2 | 0.0424 | 0.0040 | [0.0346; 0.0502] |
| Gamma random rate | φ | 23.0620 | 8.3833 | [6.6309; 39.4930] |
| | ν | 0.0885 | 0.0325 | [0.0248; 0.1523] |
| | μ_ϵ | 0.0130 | 0.0279 | [-0.0416; 0.0677] |
| | σ_ϵ^2 | 0.0424 | 0.0040 | [0.0346; 0.0502] |

Table 6 AIC and BIC values based on the LASER data

| Model | AIC | BIC |
|-------------------|---------|---------|
| IG random rate | 19.1214 | 21.9536 |
| Gamma random rate | 19.9464 | 22.7786 |

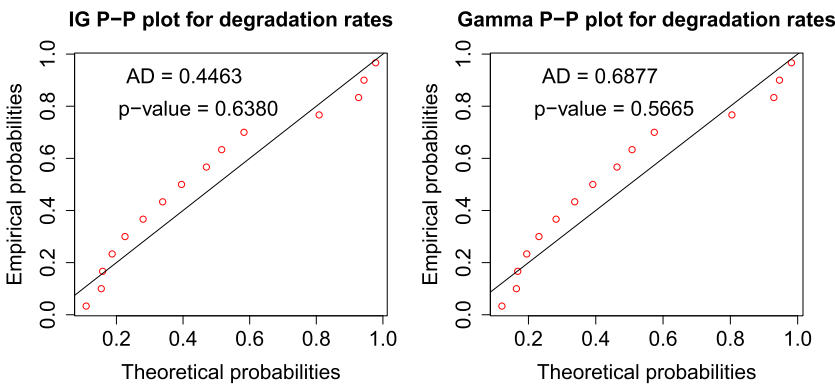


Figure 3 IG P–P plot and gamma P–P plot of the observed degradation rates based on the LASER data.

using the AD test for the gamma distribution.¹ According to the authors, this approach has satisfactory performance even for small sample sizes. Figure 3 exhibits the IG and gamma P–P plots along with the AD test for the observed degradation rates, from which we conclude that both IG and gamma random rate models are appropriate for describing the LASER degradation data (p -values > 0.05 in both cases).

Table 7 displays the lifetime 10th, 50th, and 80th percentiles and MTTF for the LASER components, from which we see that the estimated (via MLEs) lifetime percentiles and MTTF are similar to each other, and about 80% of the LASER components are supposed to have failed up to 6000 hours of operation. Such results are similar to the analysis from Meeker

¹More specifically, the authors state that, if $r_i \sim \text{IG}(\mu, \lambda)$, then $w_i = \frac{(r_i - \bar{r})^2}{r_i} \sim \text{Gamma}(\frac{1}{2}, \beta)$, where $\beta = 2\frac{\mu^2}{\lambda}$, for $i = 1, \dots, n$. Hence, testing $H_0 : r_1, \dots, r_n \sim \text{IG}(\mu, \lambda)$ is asymptotically equivalent to testing $H'_0 : w_1, \dots, w_n \sim \text{Gamma}(\frac{1}{2}, \beta)$. In this case, since the parameters are unknown, we can use the transformed observations: $w_i = \frac{(r_i - \bar{r})^2}{r_i}$, for $i = 1, \dots, n$, where $\bar{r} = \frac{1}{n} \sum_{i=1}^n r_i$ denotes the sample mean. These quantities are asymptotically independent random variables with $\text{Gamma}(\frac{1}{2}, \beta)$ distribution. Finally, the well-known Anderson–Darling test (Anderson and Darling, 1954) can be applied for testing H'_0 .

Table 7 MLEs and 95% CIs of the lifetime percentiles and MTTF based on the LASER data

| Quantity | IG random rate model | | Gamma random rate model | |
|-----------|----------------------|------------------|-------------------------|------------------|
| | MLE | 95% CI | MLE | 95% CI |
| $t_{0.1}$ | 3.8468 | [3.3088; 4.3849] | 3.8429 | [3.3373; 4.3486] |
| $t_{0.5}$ | 5.0014 | [4.4815; 5.5213] | 4.9691 | [4.4399; 5.4984] |
| $t_{0.8}$ | 5.9424 | [5.2234; 6.6614] | 5.9589 | [5.1742; 6.7435] |
| MTTF | 5.1060 | [4.5698; 5.6422] | 5.1195 | [4.5519; 5.6871] |

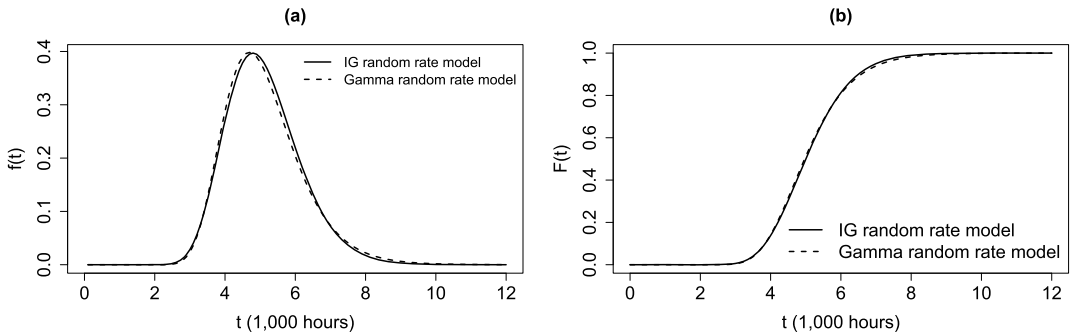


Figure 4 Lifetime distribution based on the LASER data: (a) Lifetime p.d.f., (b) Lifetime c.d.f.

and Escobar (1998), in which the 80th percentile of the pseudo lifetimes under a Weibull distribution is equal to 5932.2250 hours, whereas the MTTF is equal to 5127.8600 hours. The authors pointed out that the results obtained by the approximate method are satisfactory when the degradation paths are relatively simple.

Finally, Figure 4 shows the plots of the estimated p.d.f. and c.d.f. under the IG and gamma random rate models, from which we conclude that the p.d.f. and c.d.f. curves are similar to each other.

6.2 The locomotive wheels data

Wheel failures are responsible for much of the railroad vehicle accidents, which bring high costs to private companies and government. The railway maintenance services account for mechanical repairs of the locomotives and hold some detailed information about preventive or corrective interventions. The data set considered here is part of a study (presented by Freitas et al. (2009)) led by a Brazilian railroad company and includes the diameter, in millimeters (mm), of 14 locomotive wheels obtained from 13 inspections done up to 600,000 kilometers (km) traveled in equidistant intervals. The degradation measure for each wheel is the wear, in mm, on the wheel diameter over the traveled distance, more precisely, the difference between the actual wheel diameter and the diameter of a new wheel (966 mm) over km traveled. A wheel is considered to be not working when its degradation measure achieves 77 mm, i.e., when the wheel diameter is distant 77 mm from a new wheel. Figure 5 exhibits similar degradation paths, indicating the critical value associated with the failure. The wheels that attain the threshold remain until the next inspection when they are replaced due to preventive policies.

Table 8 displays the MLEs, SEs, and 95% CIs of the parameters under the IG random rate model (9) and the gamma random rate model (12), based on the locomotive wheels data. From this table, we conclude that the MLEs of μ_ϵ and σ_ϵ^2 are similar in both models, as well as the corresponding SEs and 95% CIs. It is worth noticing that the measurement error

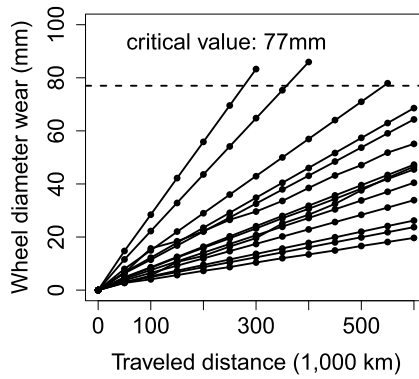


Figure 5 Degradation paths from the locomotive wheels data.

Table 8 MLEs, SEs and 95% CIs of the model parameters based on the locomotive wheels data

| Model | Parameter | MLE | SE | 95% CI |
|-------------------|-----------------------|--------|--------|------------------|
| IG random rate | μ | 0.0994 | 0.0174 | [0.0653; 0.1334] |
| | λ | 0.2324 | 0.0879 | [0.0600; 0.4048] |
| | μ_{ϵ} | 1.0331 | 0.1445 | [0.7499; 1.3164] |
| | σ_{ϵ}^2 | 0.7151 | 0.0846 | [0.5493; 0.8808] |
| Gamma random rate | φ | 2.7985 | 1.0016 | [0.8353; 4.7617] |
| | ν | 0.0355 | 0.0139 | [0.0082; 0.0628] |
| | μ_{ϵ} | 1.0331 | 0.1445 | [0.7505; 1.3171] |
| | σ_{ϵ}^2 | 0.7151 | 0.0846 | [0.5493; 0.8808] |

Table 9 AIC and BIC values based on the locomotive wheels data

| Model | AIC | BIC |
|-------------------|----------|----------|
| IG random rate | 517.9400 | 520.4970 |
| Gamma random rate | 519.7270 | 522.2840 |

distribution is offset to the right of zero, which means that the errors tend to assume positive values. For easy viewing, the distance scale is expressed in 1000 km traveled, then the MLEs of μ and λ in (9), as well as the MLE of ν in (12), have to be divided by y in practical situations.

Table 9 shows the AIC and BIC values, which both provide empirical evidence in favor of the IG random rate model. However, the difference between the AIC (BIC) value for the IG random rate model and the AIC (BIC) value for the gamma random rate model is less than two ($= 1.787$), thus indicating that both candidate models are plausible for the locomotive wheels data.

Besides, Figure 6 exhibits the IG and gamma P–P plots along with the AD adherence test of the observed degradation rates, from which we conclude that both IG and gamma random rate models are appropriate for characterizing the locomotive wheels data (p -values > 0.05 in both cases).

Furthermore, Table 10 displays the lifetime percentiles and MTTF for the locomotive wheels, and Figure 7 shows the plots of the estimated p.d.f. and c.d.f. under the IG and gamma random rate models. From Table 10, we see that the estimated lifetime percentiles and MTTF are similar to each other, and about 80% of the wheels must be switched off up to

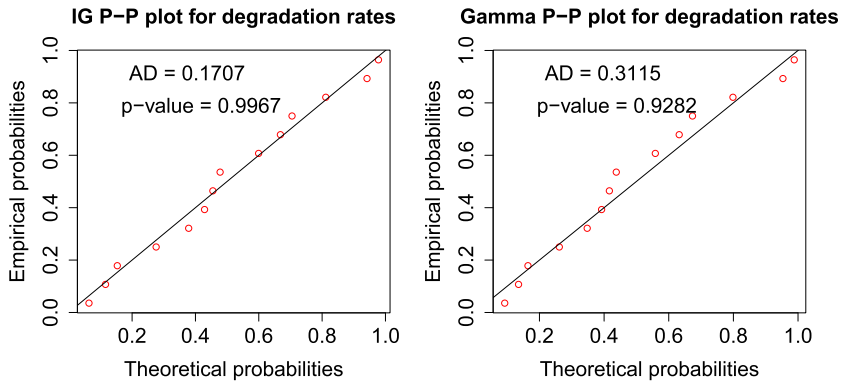


Figure 6 IG P–P plot and gamma P–P plot of the observed degradation rates based on the locomotive wheels data.

Table 10 MLEs and 95% CIs of the lifetime percentiles and MTTF based on the locomotive wheels data

| Quantity | IG random rate model | | Gamma random rate model | |
|-----------|----------------------|-------------------|-------------------------|--------------------|
| | MLE | 95% CI | MLE | 95% CI |
| $t_{0.1}$ | 430.19 | [279.91; 580.48] | 423.45 | [240.15; 606.74] |
| $t_{0.5}$ | 876.86 | [591.09; 1162.60] | 936.55 | [645.08; 1228.00] |
| $t_{0.8}$ | 1563.80 | [848.92; 2278.70] | 1559.80 | [1005.00; 2114.60] |
| MTTF | 1205.78 | [602.44; 1809.10] | 1106.24 | [744.27; 1468.20] |

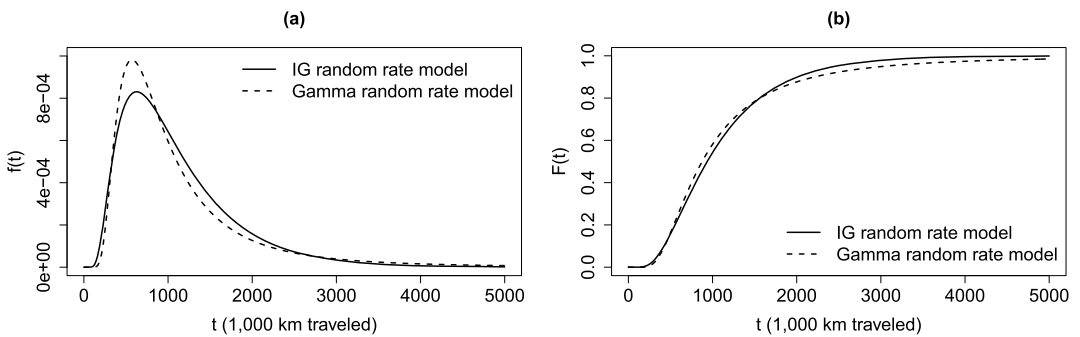


Figure 7 Lifetime distribution based on the locomotive wheels data: (a) Lifetime p.d.f., (b) Lifetime c.d.f.

1,560,000 km traveled. Moreover, from Figure 7, we see that the p.d.f. and c.d.f. curves are similar to each other.

7 Concluding remarks

In this paper, we proposed a random deterioration rate model with measurement error, in which the individual random rates follow an IG distribution. The IG random rate model takes into account the variability in the degradation data coming from different sources: the unit-varying uncertainty among different units, the temporal variability and the variability due to measurement error. Since the integrals in the likelihood function and its derivatives are intractable, we proposed to approximate it by a quadrature method and then obtain the MLEs of the model parameters. The methodology was implemented by the QUADPACK routine

(Piessens et al., 2012) along with the Quasi-Newton optimization method via the BFGS algorithm available in Ox software (Doornik, 2009). The methods showed convergence in the simulation study and the application with the real-world data sets. The simulation studies revealed that, in general, the MLEs tend to be unbiased and consistent, even when the data are perturbed by the variability of the measurement error, which means that the asymptotic intervals are adequate to use in practical situations. Besides, the simulation results demonstrated that the AIC and BIC metrics are suitable for model selection/discrimination. The application with the LASER data and the locomotive wheels data showed that the IG and gamma random rate models gave similar results, but the first one best fitted both data sets.

Future work may include considering the use of flexible measurement error models, such as the one introduced by Rondon and Bolfarine (2017), where the error term distribution belongs to the class of scale mixtures of normal distributions, which includes as particular cases the Student-t, slash, Laplace and symmetric hyperbolic distributions, among others.

Acknowledgments

We are grateful to the anonymous referees and the editor for the very useful comments and suggestions, which greatly improved this paper. F. Louzada was partially supported by CNPq, FAPESP. Pedro L. Ramos acknowledges support from the São Paulo State Research Foundation (FAPESP Proc. 2017/25971-0).

Supplementary Material

Supplement to “The random deterioration rate model with measurement error based on the inverse Gaussian distribution” (DOI: [10.1214/20-BJPS468SUPP](https://doi.org/10.1214/20-BJPS468SUPP); .zip). The supplementary material exhibits the routine in Ox software to estimate the parameters and also the code in R software to generate the graphs.

References

- Anderson, T. W. and Darling, D. A. (1954). A test of goodness of fit. *Journal of the American Statistical Association* **49**, 765–769. [MR0069459](https://doi.org/10.1080/01621459.1954.10501459)
- Broyden, C. G. (1970). The convergence of a class of double-rank minimization algorithms. *Journal of the Institute of Mathematics and Its Applications* **6**, 76–90. [MR0433870](https://doi.org/10.1093/jim/6.1.76)
- Burnham, K. P. and Anderson, D. R. (2002). *Model Selection and Multimodel Inference: A Practical Information-Theoretic Approach*, 2nd ed. New York, NY. [MR1919620](https://doi.org/10.1002/9781118133216)
- Carrasco, J. M. F., Ferrari, S. L. P. and Arellano-Valle, R. B. (2014). Errors-in-variables beta regression models. *Journal of Applied Statistics* **41**, 1530–1547. [MR3292031](https://doi.org/10.1080/02664763.2014.881784) <https://doi.org/10.1080/02664763.2014.881784>
- Crowther, M. J., Andersson, T. M.-L., Lambert, P. C., Abrams, K. R. and Humphreys, K. (2016). Joint modelling of longitudinal and survival data: Incorporating delayed entry and an assessment of model misspecification. *Statistics in Medicine* **35**, 1193–1209. [MR3476536](https://doi.org/10.1002/sim.6779) <https://doi.org/10.1002/sim.6779>
- Doornik, J. A. (2009). An object-oriented matrix programming language ox 6.
- EPRI (2006). Steam generator integrity assessment guidelines: REVISION 2. Technical Report TR1012987.
- Fenyvesi, L., Lu, H. and Jack, T. R. (2004). Prediction of corrosion defect growth on operating pipelines. In *2004 International Pipeline Conference*, 225–230. American Society of Mechanical Engineers.
- Freitas, M. A., Luíza, M., de Toledo, G., Colosimo, E. A. and Pires, M. C. (2009). Using degradation data to assess reliability: A case study on train wheel degradation. *Quality and Reliability Engineering International* **25**, 607–629.
- Freitas, M. A., Colosimo, E. A., dos Santos, T. R. and Pires, M. C. (2010). Reliability assessment using degradation models: Bayesian and classical approaches. *Pesquisa Operacional* **30**, 194–219.
- Huysse, L. and Roodselaar, V. (2010). Effects of inline inspection sizing uncertainties on the accuracy of the largest features and corrosion rate statistics. In *2010 8th International Pipeline Conference (IPC2010)*. Calgary, Alberta, Canada.

- Kass, R. E. and Steffey, D. (1989). Approximate Bayesian inference in conditionally independent hierarchical models (parametric empirical Bayes models). *Journal of the American Statistical Association* **84**, 717–726. MR1132587
- Lesaffre, E. and Spiessens, B. (2001). On the effect of the number of quadrature points in a logistic random effects model: An example. *Journal of the Royal Statistical Society Series C Applied Statistics* **50**, 325–335. MR1856328 <https://doi.org/10.1111/1467-9876.00237>
- Liu, L. and Yu, Z. (2008). A likelihood reformulation method in non-normal random effects models. *Statistics in Medicine* **27**, 3105–3124. MR2522152 <https://doi.org/10.1002/sim.3153>
- Lu, C. J. and Meeker, W. Q. (1993). Using degradation measures to estimate a time-to-failure distribution. *Technometrics* **35**, 161–174. MR1225093 <https://doi.org/10.2307/1269661>
- Meeker, W. Q. and Escobar, L. A. (1998). *Statistical Methods for Reliability Data*. New York, NY: John Wiley & Sons. Chapter 13.
- Meeker, W. Q., Escobar, L. A. and Lu, C. J. (1998). Accelerated degradation tests: Modeling and analysis. *Technometrics* **40**, 89–99.
- Morita, L. H. M., Tomazella, V. L. D., Ramos, P. L., Ferreira, P. H. and Louzada, F. (2020). Supplement to “The random deterioration rate model with measurement error based on the inverse Gaussian distribution.” <https://doi.org/10.1214/20-BJPS468SUPP>
- Nelson, K. P., Lipsitz, S. R., Fitzmaurice, G. M., Ibrahim, J., Parzen, M. and Strawderman, R. (2006). Use of the probability integral transformation to fit nonlinear mixed-effects models with nonnormal random effects. *Journal of Computational and Graphical Statistics* **15**, 39–57. MR2269362 <https://doi.org/10.1198/106186006X96854>
- Pandey, M. D. and Lu, D. (2013). Estimation of parameters of degradation growth rate distribution from noisy measurement data. *Structural Safety* **43**, 60–69.
- Peng, C. Y. and Tseng, S. T. (2009). Mis-specification analysis of linear degradation models. *IEEE Transactions on Reliability* **58**, 444–455.
- Peng, W., Li, Y.-F., Yang, Y.-J., Huang, H.-Z. and Zuo, M. J. (2014). Inverse Gaussian process models for degradation analysis: A Bayesian perspective. *Reliability Engineering & Systems Safety* **130**, 175–189.
- Piessens, R., de Doncker-Kapenga, E., Überhuber, C. W. and Kahaner, D. K. (2012). *Quadpack: A Subroutine Package for Automatic Integration, Vol. 1*. Berlin: Springer. MR0712135 <https://doi.org/10.1007/978-3-642-61786-7>
- Pinheiro, J. C. and Bates, D. M. (1995). Approximations to the log-likelihood function in the nonlinear mixed-effects model. *Journal of Computational and Graphical Statistics* **4**, 12–35.
- R Core Team R (2018). *A Language and Environment for Statistical Computing; 2015*.
- Raftery, A. E. (1995). Bayesian model selection in social research. *Sociological Methodology* **25**, 111–163.
- Rondon, L. M. and Bolfarine, H. (2017). Bayesian analysis of flexible measurement error models. *Brazilian Journal of Probability and Statistics* **31**, 618–639. MR3693983 <https://doi.org/10.1214/16-BJPS326>
- Sakamoto, Y., Ishiguro, M. and Kitagawa, G. (1986). *Akaike Information Criterion Statistics, Vol. 1*, 1st ed. Netherlands: Springer. MR0876486
- Schwarz, G. (1978). Estimating the dimension of a model. *The Annals of Statistics* **6**, 461–464. MR0468014
- Seshadri, V. (2012). *The Inverse Gaussian Distribution: Statistical Theory and Applications, Vol. 137*. Berlin: Springer. MR1622488 <https://doi.org/10.1007/978-1-4612-1456-4>
- van Noordwijk, J. M. (2009). A survey of the application of gamma processes in maintenance. *Reliability Engineering & Systems Safety* **94**, 2–21.
- Villaseñor, J. A. and Gonzalez-Estrada, E. (2015). Tests of fit for inverse Gaussian distributions. *Statistics & Probability Letters* **105**, 189–194. MR3371998 <https://doi.org/10.1016/j.spl.2015.06.017>
- Wang, X. and Xu, D. (2010). An inverse Gaussian process model for degradation data. *Technometrics* **52**, 188–197. MR2676425 <https://doi.org/10.1198/TECH.2009.08197>
- Xiao, N.-C., Huang, H.-Z., Wang, Z., Liu, Y. and Zhang, X.-L. (2012). Unified uncertainty analysis by the mean value first order saddlepoint approximation. *Structural and Multidisciplinary Optimization* **46**, 803–812.

L. H. M. Morita
 Department of Statistics
 Federal University of Mato Grosso
 Cuiabá, MT
 Brazil
 E-mail: liamorita@ufmt.br

V. L. D. Tomazella
 Department of Statistics
 Federal University of São Carlos
 São Carlos, SP
 Brazil

P. L. Ramos
P. H. Ferreira
F. Louzada
Institute of Mathematical and Computer Sciences
University of São Paulo
São Carlos, SP
Brazil
E-mail: pedrolramos@usp.br
paulohenri@ufba.br
louzada@icmc.usp.br